

**Simulation Tool for Third-party Vendors Using Apple's Watch
Charger WPT Module**

FCC §2.1093

Revision history

Revision	Date	Description
1.0.0	December 2022	Initial Release of SAR Simulation API tool to support Apple's Watch Charger WPT Module .
1.0.1	March 2023	Added response to FCC questions received on 1 st March, 2023

Table of Contents

1	Introduction	6
1.1	WPT Watch Charger Module :.....	6
2	Wireless Power Transfer System	11
3	Apple’s Simulation Model Validation Methodology.....	12
3.1	Simulation Model Validation Study	13
3.1.1	H-field Simulations.....	13
3.1.2	H-field Measurements.....	14
3.1.3	Simulation Vs Measurement Comparison	15
4	Total Computational Uncertainty.....	17
5	Third-Party Vendor’s SAR Simulations Methodology.....	21
5.1	Validation of Watch Charger Simulation Model	22
5.2	SAR Simulations.....	23
5.3	SAR Compliance Results:.....	24
5.3.1	Additional Exposure Cases:	24
6	Summary	25
7	Annex A: Specific Information for SAR Computational Modelling	25
8	Annex B: Algorithm Validation and Benchmarks	30
9	Annex C: Human Tissue Modeling.....	38
	FCC Communication	42

List of Figures:

Figure 1: Cross-section view of Watch Charger Module..... 7

Figure 2: WPT Module (a) Trimetric View (b) Bottom View with Pin-out Description (c) Side View 7

Figure 3: Workflow of the Apple Watch Charger WPT Simulation..... 10

Figure 4: Overview of Model Validation 12

Figure 5: Detailed Workflow of Apple’s Simulation Model Validation 13

Figure 6: Demonstration of the Watch and the Charger placement. 14

Figure 7: Example to demonstrate H-field measurement using Near-field EMI probes [1]..... 15

Figure 8: Scanning EUT to Measure H-field spatially..... 15

Figure 9: Simulated Vs Measured H-field when the probe moves away from touching the Charger ($z=0$) to 20 cm. 17

Figure 10: Vendor’s Simulation Workflow for Computational Exposure Assessment 21

Figure 11: Sample Field Plots to Show the Field Data Comparison Between Two Plots 22

Figure 12: Example to Demonstrate the Working of API Interface 23

Figure 13: Phantom Dimensions 27

Figure 14: Adaptive Meshing in HFSS 27

Figure 15: Simulated Vs Measured Correlation of Transmitter model..... 28

Figure 16: Mesh Seeding on Phantom 29

Figure 17: IEEE P1528.4 for SAR Computation 30

Figure 18: Electrical Properties of (a) Bone, (b) Muscle, and (c) Dry Skin 40

List of Tables:

Table 1. Key Design Parameters	11
Table 2. Charging Profile/Sequence.....	11
Table 3. Comparison of the simulated and measured H-field.....	16
Table 4. Budget of Uncertainty Contributions of the Numerical Algorithm	18
Table 5. Measurement Uncertainty Table	19
Table 6. Expanded Standard Uncertainty.....	20
Table 7. Material Properties and Tolerances.....	20
Table 8. List of inputs to API interface.....	23
Table 9. List of Computational Parameters.....	25
Table 10. Tx and Rx Coil Parameters	26
Table 11. Electrical Properties for Body Layers	38
Table 12. Electrical Properties of Human Hand Layers.....	38

1 Introduction

Apple is planning to enable third-party vendors to design their own external housing using Apple's Watch Charger Wireless Power Transfer (WPT) module design. The finished WPT products will bear their own FCC IDs under the third-party vendors' names. No change to the WPT design can be made by the approved vendors but they can design with their own form factors and housing materials. This document describes how vendors can utilize a SAR simulation model developed and provided by Apple to demonstrate RF exposure compliance for near-body portable use conditions.

The Watch Charger WPT module operates at two charging frequencies 326 kHz and 1.778 MHz is proprietarily designed by Apple and will be supplied to approved third-party vendors wherein the vendors can add their custom housing geometries for different desktop or portable applications. While E/H field measurements are relatively accessible to those vendors, they often lack the resources or expertise to conduct SAR simulation for portable WPT devices or mixed mobile/portable devices when used near body. Therefore, a SAR simulation tool has been developed by Apple to allow vendors to conduct SAR simulations after entering form factor related parameters.

To demonstrate RF exposure compliance for Portable devices, as permitted by §2.1093 (certification for portable devices below 4 MHz), SAR numerical simulations are performed to demonstrate compliance to the 1.6 W/kg localized 1-g SAR limit.

Apple, with joint collaboration from Ansys Inc., has developed an API interface which allows vendors to perform complex SAR simulations for the WPT charger module. SAR Compliance report will be automatically generated by the simulation tool. A "FCC_Vendor_sample_report" is attached.

Any updates/changes to the simulation software and the API can only be done by Apple working together with Ansys.

1.1 WPT Watch Charger Module :

Apple's WPT Watch Charger consists of a tightly wound copper coil. Currently, it is only used for charging Watches. Magnets are used to attach the Watch to the vendor's WPT Watch charger module to provide wireless charging up to 2.8W. The cross-section view of the charger is shown in Fig. 1. The charger module is shielded on the bottom with Aluminum, As shown in Fig. 2, in the bottom enclosure, 3 pins are exposed for connection to the vendor's design: a) PWR b) COIL+, and c) COIL -

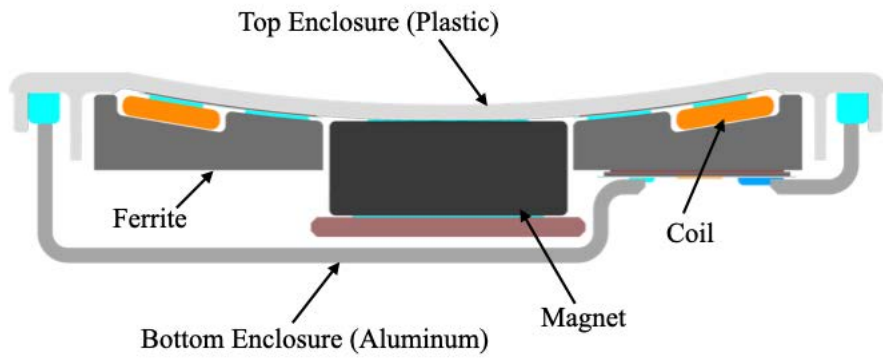


Figure 1: Cross-section view of Watch Charger Module

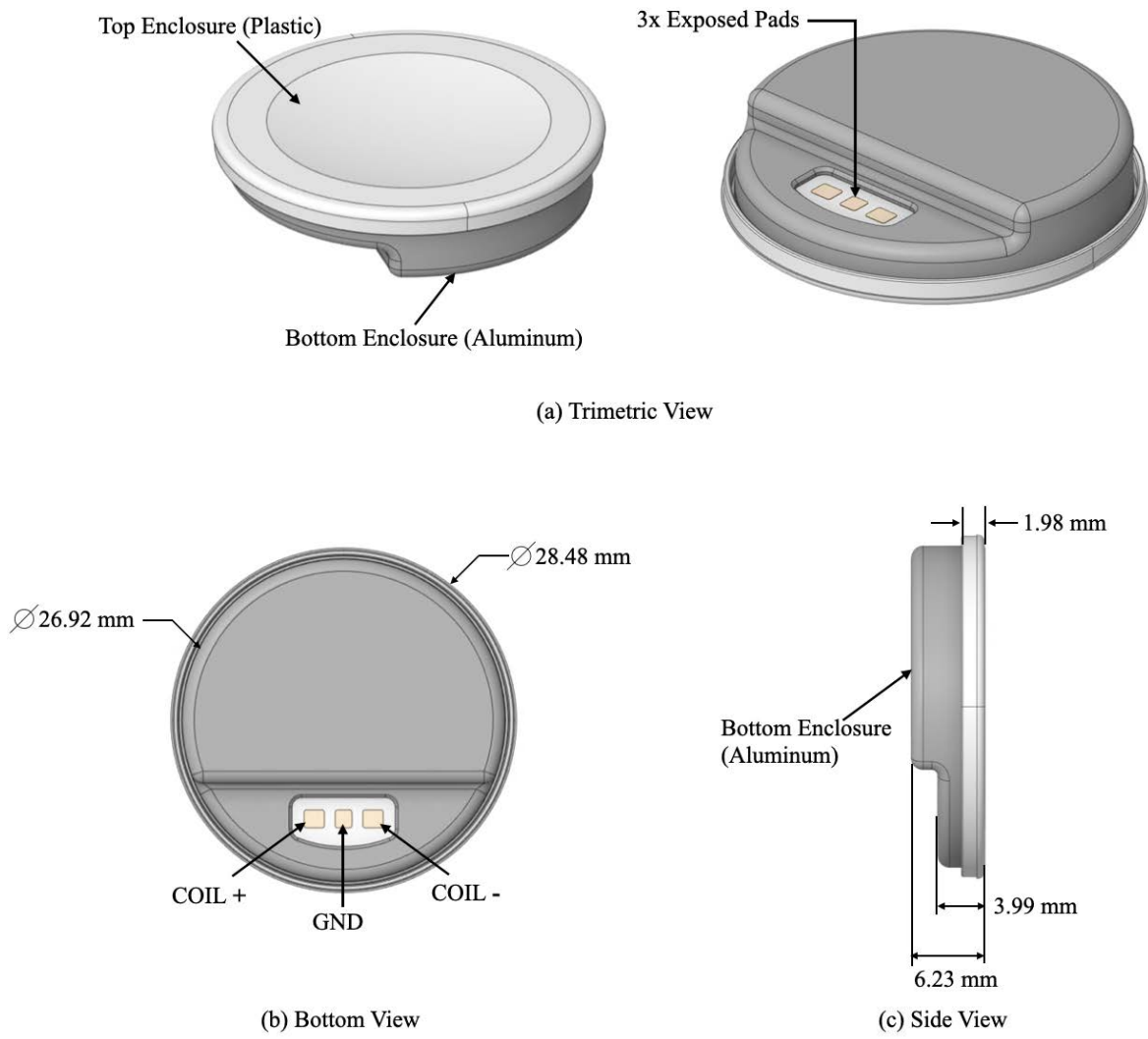


Figure 2: WPT Module (a) Trimetric View (b) Bottom View with Pin-out Description (c) Side View

Apple will supply these charger modules to approved third-party vendors. Vendors do not have access to the design or firmware. Therefore, no change is allowed. Vendors can only add cable routings through the exposed pads and their custom form factor design.

To enable third-party vendors with SAR simulation capability to address portable use conditions, if applicable, Apple has created the workflow/instruction described below and is illustrated in Fig. 3. Apple takes the responsibility of creating the simulation model and has validated it with measurements as shown in later sections.

Instruction to vendors for the use of Apple's Watch Charger WPT simulation model, including applicability and restrictions, are outlined as follow:

- i. Vendors cannot modify the WPT module or the simulation model, only external geometry and material property can be added.
- ii. Supports wireless power transfer for only Apple Watches at 326 kHz and 1.778 MHz charging frequency.
- iii. Allows for wireless power transfer between one source (single primary coil) and one client (single secondary coil) at any given time and maximum output power supported is up to 2.8 W.
- iv. Supports only portable SAR simulations at 0 mm. The worst case evaluation can hence cover all use case scenarios such as head, body, extremity, and desktop cases.
- v. Vendors designing WPT charger system with capability to charge multiple Apple devices such as Apple iPhone plus Apple Watch and/or AirPods, can use this WPT simulation model to perform simulations for Apple Watch use case only. Vendors are responsible for addressing compliance of other WPT client devices (Apple iPhone, AirPods, or concurrent multiple iPhones).
- vi. Vendors shall use the same FEM (Finite Element Method) software which has been validated by Apple. Any update/change to software can only be issued by Apple.
- vii. Currently this simulation tool supports only Apple Watches as client device for wireless charging at 326 kHz and 1.778 MHz and only the following exposure cases are simulated:
 - a) nominal placement: represents normal use condition.
 - b) Unrealistic scenario: no Rx is present.

In the future, we may extend the capability of this model to add:

- a) support for other Rx devices (for example: AirPods);
- b) support additional charging frequencies;
- c) additional exposure cases.

Regulatory approval will be obtained by Apple before release of the above future features or any changes to the software that degrades the characteristics reported in this document.

Along with the Watch Charger WPT simulation model, the following information will be provided to the third-party vendors:

- i. reference Electric (E) and Magnetic (H) simulations field data to verify the vendor's simulation system;
- ii. final uncertainty value from uncertainty analysis study.

As an initial step, vendors shall run the Watch Charger WPT simulation software and verify simulated E/H results against Apple provided E/H reference data to make sure that the vendor's simulation system is working correctly. This step will also ensure the vendor is using all the correct simulation settings and eliminates the need to run uncertainty analysis and code verification which have been already performed by Apple. Any discrepancy with the reference E/H field data should be analyzed and corrected. After validation of the simulation model, vendors can enter their custom housing parameters to perform computational SAR assessment.

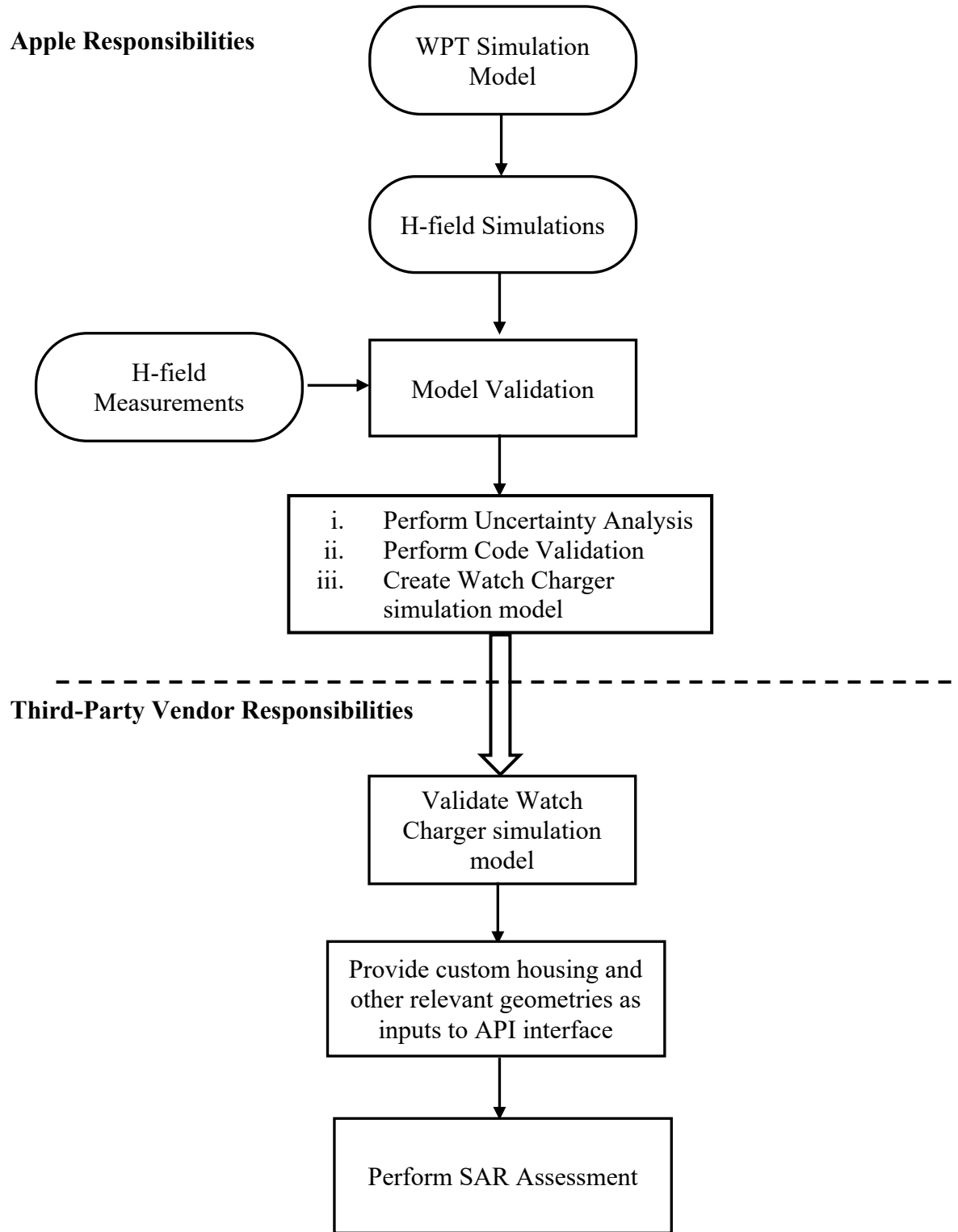


Figure 3: Workflow of the Apple Watch Charger WPT Simulation

2 Wireless Power Transfer System

The wireless power transfer system consists of a transmitting coil with 9 turns and measures 2.35 uH nominally in free air. The receiver coil on the client side consists of 6 turns and measures 7.55 uH nominally in free air. Both coils are wound spirally and made of stranded wire.

Below Table 1 lists the key design parameters:

Table 1. Key Design Parameters

Item	Description
Max Power Delivered	2.8 W (delivered to battery)
Full Charge Time	1 hour 9 minutes (from empty)
Operating Frequency	326 kHz , 1.778 MHz
Communications/Modulation Method	ASK from Watch to Charger FSK from Charger to Watch
Object Detection Mode	Low Power Efficiency test

The target power which is defined as the maximum deliverable power to the receiver (Watch) by the transmitter, is impacted by the coupling efficiency between the transmitter and the receiver coils. Under nominal conditions, maximum power of 2.8 W can be delivered to the receiver. Below is the charging profile/sequence.

Table 2. Charging Profile/Sequence

Battery State of Charge	Charge Duration in min	Power Delivered to rectifier in Watts
0-10%	11	0.6 W
10-50%	15	2.8 W
50-100%	43	Changes from 2.8 W to 0.2 W

During Object Detection Mode (ODM), the charging device will detect the object (Watch) via low power efficiency test. If the efficiency metric is below a specified threshold, then the external object is identified as a foreign object and charging session will not be initiated. Only when an intended Rx (Watch) device is placed on the Charger, communication link will be established with the Rx device and power transfer can begin. Charging will stop whether the Rx is fully charged, or the user removes the client from the charging device, causing a communications loss.

3 Apple's Simulation Model Validation Methodology

The following steps have been taken to show the validity of the model used for SAR simulations:

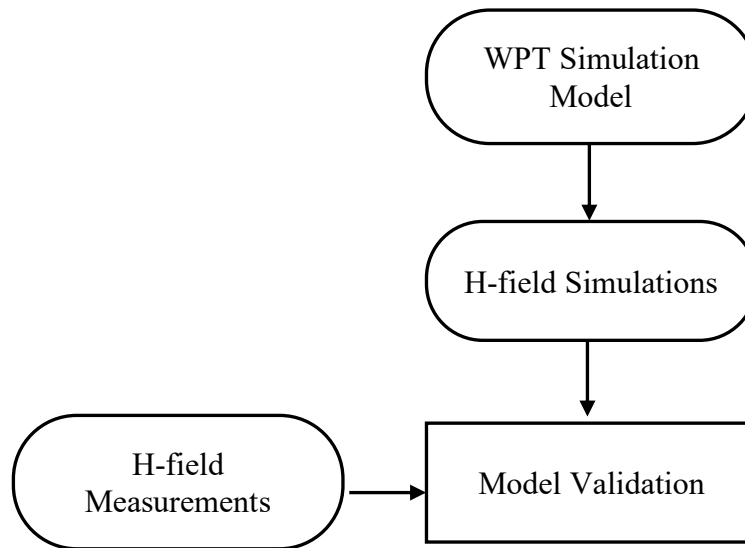


Figure 4: Overview of Model Validation

- 1) EM Simulation:
 - a. Import a CAD model that represents the actual product in the simulation tool.
 - b. Define material properties inside the product based on vendor's inputs.
 - c. Extract two-port network impedance matrix ($[Z]$) from the simulation.
- 2) Circuit Simulation:
 - a. Include the impedance matrix in the wireless power transfer (WPT) circuit model.
 - b. Run circuit simulation and extract coils' current waveforms.
- 3) Field, H-field, and SAR Calculations:
 - a. Use the current waveforms to drive the EM simulation model.
 - b. Calculate H-field from simulation.
 - c. Compare simulated H-field with measured H-field.

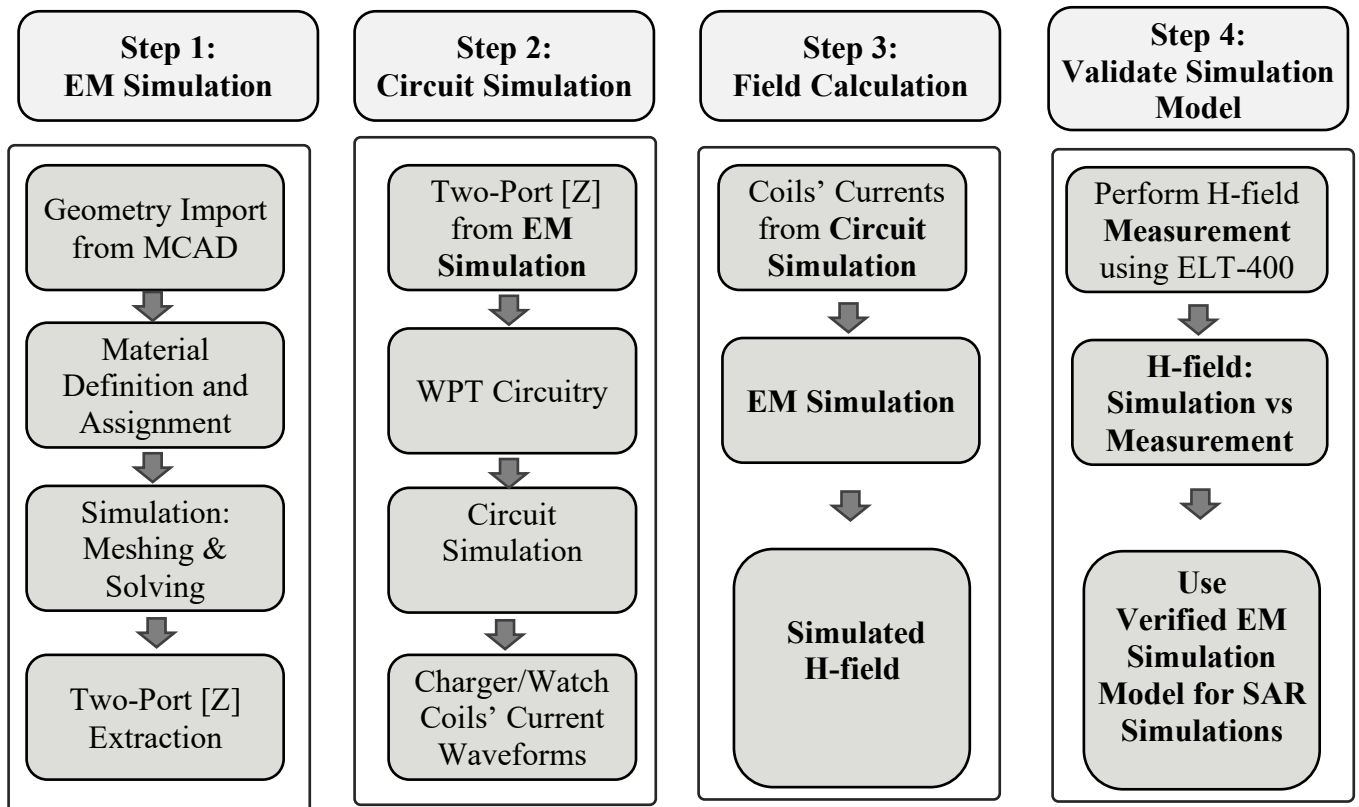


Figure 5: Detailed Workflow of Apple's Simulation Model Validation

3.1 Simulation Model Validation Study

To validate the simulation model, measurements are made on the EUT and compared to the simulated model results. H-field measurements are performed to verify the simulation model's accuracy versus measurement results. Only a validated simulation model will be used for SAR simulations.

3.1.1 H-field Simulations

Electromagnetics simulations are conducted using commercially available software Ansys HFSS. For the simulations, following Step 1, which is described above, the CAD file that represents the EUT is first imported. Ansys is a CAD agnostic tool and accepts most of the CAD formats (e.g., step) with minimal requirements for CAD cleaning. Then, the proper material properties are assigned at the operating frequency (e.g., 326 kHz / 1.778 MHz). A proper mesh seeding is performed, and ports are assigned. After 3D simulation is completed, as mentioned in Step 2, the two-port network [Z] data was extracted and used with the WPT circuit model. This WPT model

includes the charger source as well as the watch side rectifier circuit. Solving using a circuit tool (e.g., Ansys Simplorer tool), proper excitations for transmitter (charger) and receiver (watch) coils are calculated. Later, in Step 3, these current waveforms are fed into the Ansys HFSS to excite the coils and create H-field. During the Step 4, a set of measurements will be conducted to verify the simulation model's accuracy versus measurement results. The computational uncertainty will be used to judge the model accuracy. After the model passed the verification, it will be used for SAR simulations.

Below figure shows the placement of the watch and charger during operating condition.

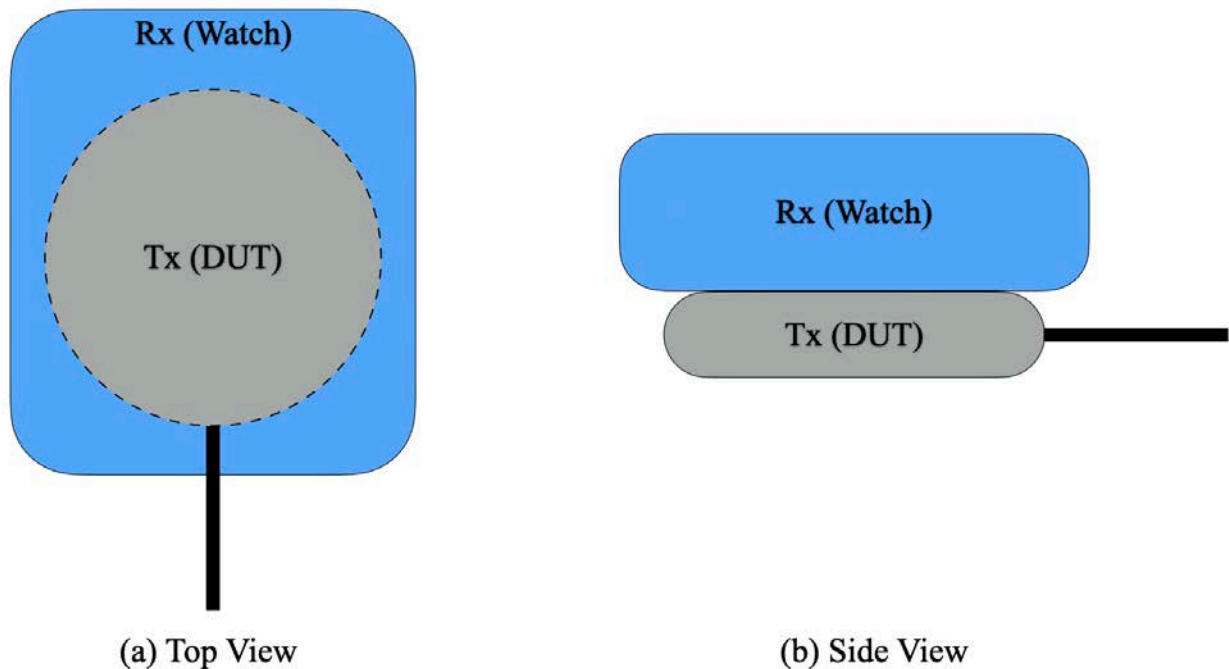


Figure 6: Demonstration of the Watch and the Charger placement.

3.1.2 H-field Measurements

Near-field EMI Low Frequency Probes available from Amber Precision Instruments (API) are used for H-field measurements [1]. These probes pick up the fields at near-field regions and give us the flexibility to measure fields very close to the EUT. To perform the near-field H-field measurements, we used 2mm H-field probes i) Hx/Hy measurement and ii) Hz probe. An example is shown in Fig. Using the SmartScan software available from API, scan area around the EUT is defined and H-field measurements are performed. A single (Hx/Hy) probe is used to measure both Hx and Hy components and a separate probe is used for Hz measurement. Later, the three x, y, and z components of the field are merged to get the final H-field value.

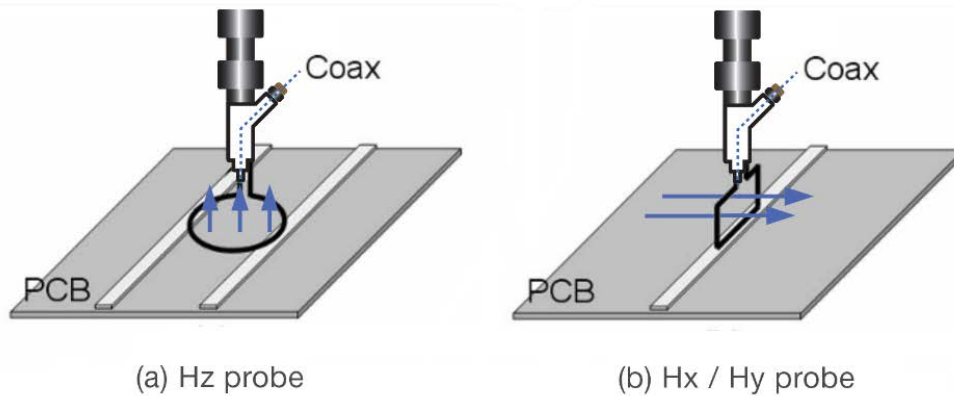


Figure 7: Example to demonstrate H-field measurement using Near-field EMI probes [1]

3.1.3 Simulation Vs Measurement Comparison

Correlation study between the simulation model and the measurements (H-field) is presented in this section. Simulation and measurement results are compared for the watch and charger side below. The target power shows the maximum deliverable power per each case.

For each side, the H-field probe is in contact with the EUT and maximum RMS H-field is reported in the tables. There is a good correlation between the simulation and measurement results.

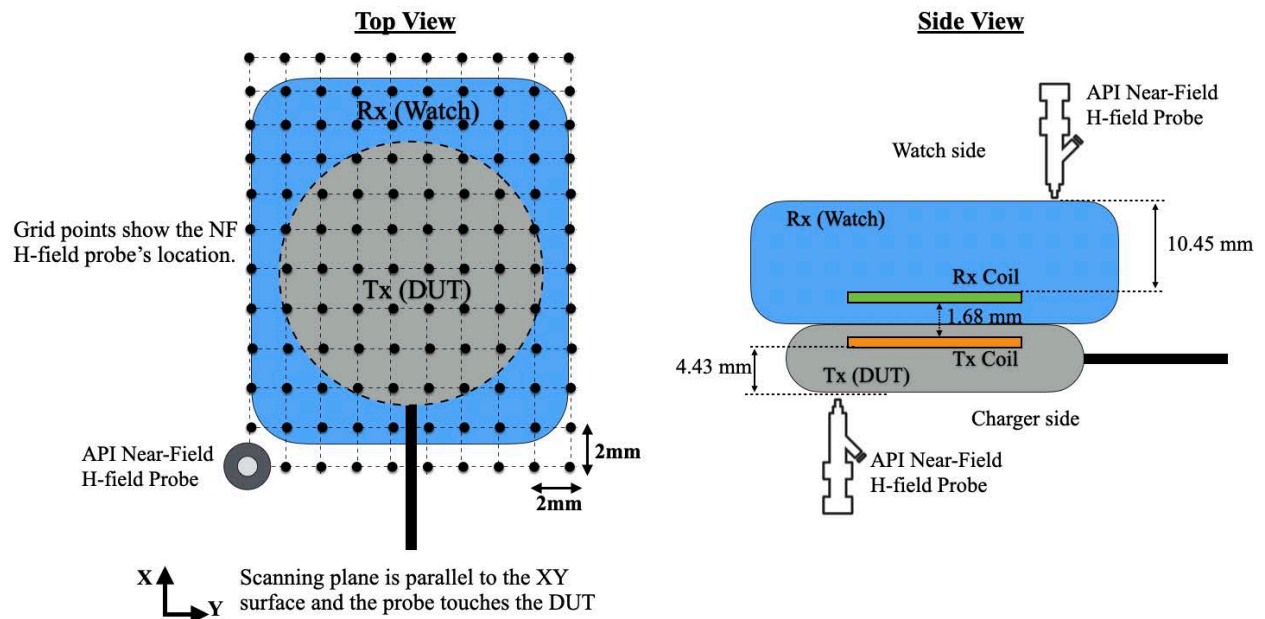


Figure 8: Scanning EUT to Measure H-field spatially

Table 3. Comparison of the simulated and measured H-field.

Simulated and Measured H-field during WPT operation at 326 kHz and 1.778 MHz

Operating condition:	Measurement Side	Power delivered to Rx (W)	Simulated RMS H-field (A/m)	Measured H-field (A/m)
Charging @ 326 kHz	Watch side	2.8	0.71	0.42
	Charger side		4.14	2.95
Charging @ 1.778 MHz	Watch side	2.8	0.75	0.66
	Charger side		4.3	3.2

Transmitter (EUT) Correlation Study:

To further evaluate the simulation model, To further evaluate the simulation model, we simulated and measured the charger only scenario using the measurement setup shown in the inset of Fig. 9. Simulation model and measurements correlation is performed at a vertical distance away from the EUT and the probe is moved vertically in Z direction from 0 mm to 20 cm.

Below Fig. 9 shows good correlation between the measurements and simulations, verifying the accuracy of the model. At distance very close to the EUT, simulations are little more conservative than measurements.

Simulated Vs Measured H-field Comparison

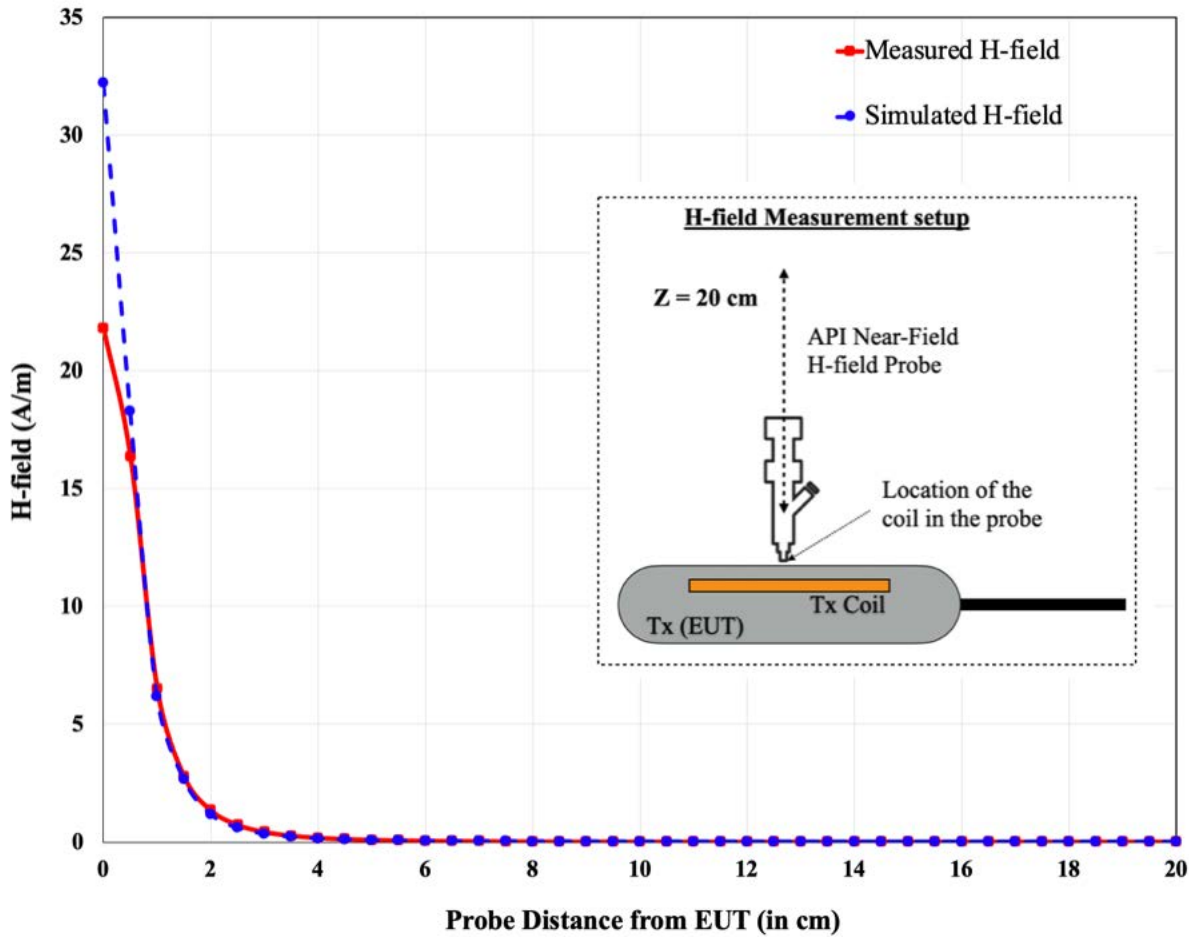


Figure 9: Simulated Vs Measured H-field when the probe moves away from touching the Charger (z=0) to 20 cm.

From both the above studies, we see that there is good correlation between simulation model and measurements and hence this validated model can be used for SAR simulations.

4 Total Computational Uncertainty

For the computational uncertainty simulations, the extreme cases where the phantom is placed directly in contact with the EUT is considered. In the following a detail description for calculating each table entity is listed. Anywhere we mention SAR deviation, it is defined as $SAR_{Deviation} \% = 100 \times [SAR_{Baseline} - SAR_{UI}] / SAR_{Baseline}$. $SAR_{Baseline}$ refers to the peak averaged spatial SAR calculated for the baseline and SAR_{UI} refers to the peak averaged spatial SAR calculated for each under investigation case.

ABC:

For this case, we could not follow the guideline one by one because the frequency is very low and moving the absorbing box by quarter wavelength means moving it by several hundred meter which is not practical. Instead, we scaled the absorbing box by different amounts (e.g., 150%) and reported the SAR deviation.

Convergence:

We added two extra adaptive passes over the baseline. We obtained the max E field locations and values inside the phantom. We made sure the max E field location in the two last passes are on the same mesh cell. Then, the highest deviation of the max E in the last 2 passes compared to the mean E field was calculated and reported.

Mesh:

Since Ansys HFSS allows for the adaptive meshing, we followed the instruction and added extra passes over the baseline case, until the total number of the mesh elements was 20% more than the total number of the mesh elements in the solved baseline case. Then, we calculated the SAR deviation.

Phantom Dielectrics:

We varied phantom dielectric properties as instructed within a defined range and calculated SAR deviation for four cases and reported the worst deviation.

Power Budget:

We calculated the input power to the system at the port. Also, calculated total loss by summing all the ohmic, dielectric, and radiation power losses. Then, calculated the power deviation using:
$$\text{PowerDeviation \%} = 100 \times [P_{\text{Input}} - P_{\text{Loss}}]/P_{\text{Input}}$$

Uncertainty of EUT model (Based on Near Field Distribution):

We used H field values from measurement and simulation (when the probe was in contact with the EUT) and calculated the deviation using: $100 \times (H_{\text{Meas}} - H_{\text{Sim}})/H_{\text{Meas}}$.

Uncertainty of Measurement Equipment and Procedure:

We extracted this number from the probe data sheet.

Below is a table summarizing the budget of the uncertainty contributions of the numerical algorithm and of the rendering of the simulation setup. The table was filled using the IEC 62704-4 ED1 from 2018.

For the simulations, the nominal operating case at 1.778 MHz where the phantom is placed directly in front of the charger is considered.

Table 4. Budget of Uncertainty Contributions of the Numerical Algorithm

a	b	d	e	g
Uncertainty component	Subclause	Probability distribution	Divisor f(d, h)	Uncertainty %
Mesh resolution	7.2.3	N	1	0.14
ABC	7.2.4	N	1	0.11
Power budget	7.2.5	N	1	0.1
Convergence	7.2.6	R	1,73	0.1
Phantom dielectrics	7.2.7	R	1,73	0.05
Combined standard uncertainty ($k = 1$)				0.5

Below is a table summarizing the budget of the uncertainty of the developed model. The table was filled using the IEC 62704-4 ED1.

Table 5. Measurement Uncertainty Table

a	b	d	e	g
Uncertainty component	Subclause	Probability distribution	Divisor f(d, h)	Uncertainty %
Uncertainty of the EUT model (based on near field distribution)	7.2.2	N	1	5.2
Uncertainty of the measurement equipment and procedure	7.2.3	N	1	5
Combined standard uncertainty ($k = 1$)				10.2

The expanded ($k = 2$) uncertainty result as per the IEC/IEEE 62704-1/-4 is listed in Table 8. The expanded standard uncertainty is 20.4, which is lower than the limit of 30.

Table 6. Expanded Standard Uncertainty

a	b	c	d	e	f	g	h
Uncertainty component	Sub clause	Tolerance %	Probability distribution	Divisor f(d,h)	c_i	Uncertainty %	ν_i or ν_{eff}
Uncertainty of the test setup with respect to simulation parameters	7.2		N	1	1	0.5	
Uncertainty of the developed numerical model of the test setup	7.3		N	1	1	10.2	
Combined standard uncertainty ($k = 1$)						10.7	
Expanded standard uncertainty ($k = 2$)						21.4	
Columns c, g and h are filled based on the results of Table 6 and Table 7							
NOTE 1 Column headings a to h are given for reference							
NOTE 2 Abbreviation used in Table							
N – normal probability distribution							
NOTE 3 The divisor is a function of the probability distribution and degrees of freedom (ν_i and ν_{eff})							
NOTE 4 c_i is the sensitivity coefficient that is applied to convert the variability of the uncertainty component into a variability of SAR							

The properties of the key materials of the EUT, as well as their tolerances, are listed in the following table.

Table 7. Material Properties and Tolerances

	Permittivity +/- Tolerance	Permeability +/- Tolerance	Loss Tangent +/- Tolerance	Conductivity +/- Tolerance
TX Ferrite	1	1000 +/-100	0	0
RX Ferrite	1	3300 +/-825	0	0
TX Coil	1	1	0	5.8e7 +/- 5.8e5
RX Coil	1	1	0	5.8e7 +/- 5.8e5
TX Shield	1	1	0	5.8e7 +/- 5.8e5
RX Shield	1	1	0	5.8e7 +/- 5.8e5

After the model validation is established, Watch Charger model with all the WPT module parameters is created and it has the following advantages:

- a) Protecting IP: All the confidential geometry details can be hidden to protect the IP and still the vendors we will be able to run all the simulations, plot E/H, SAR fields etc... and can perform all the necessary post-processing operations.
- b) Prevent Vendors to make any internal hardware changes to Apple's WPT module: Vendors cannot modify WPT module parameters such coil radius, thickness or any of the WPT parameters. Vendors can only provide the custom housing geometry with appropriate material properties as input to the API interface.

5 Third-Party Vendor's SAR Simulations Methodology

Below figure describes the Vendor workflow for computing SAR.

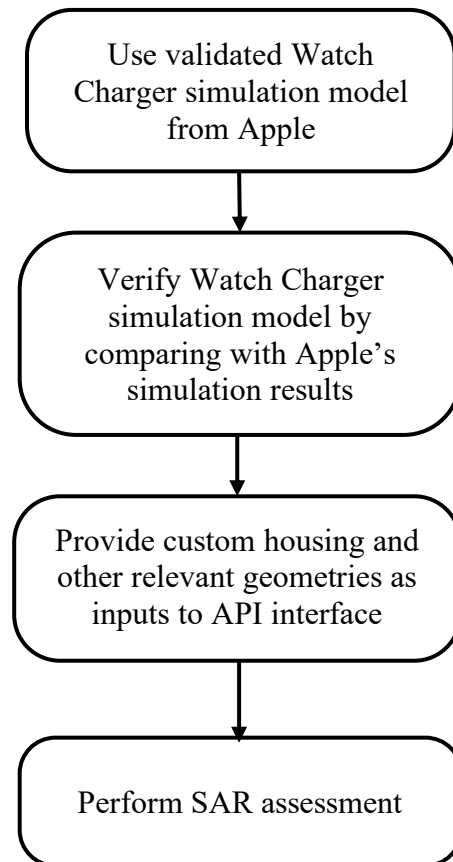


Figure 10: Vendor's Simulation Workflow for Computational Exposure Assessment

5.1 Validation of Watch Charger Simulation Model

As an initial step, third-party vendors will validate the Watch Charger simulation model provided by Apple to make sure that the simulation setup is consistent with Apple's simulation model. Vendors are going to run the Watch Charger model as-is without any modifications and verify with simulated E/H results with the E/H simulation field data provided by Apple to make sure that the shared Watch Charger model is working as expected.

Average error between both the simulation results is computed by comparing the field data values as shown below. Difference between the field data values for each grid cell are computed for the Apple's simulated data and the Watch Charger simulation model and the average error is reported.

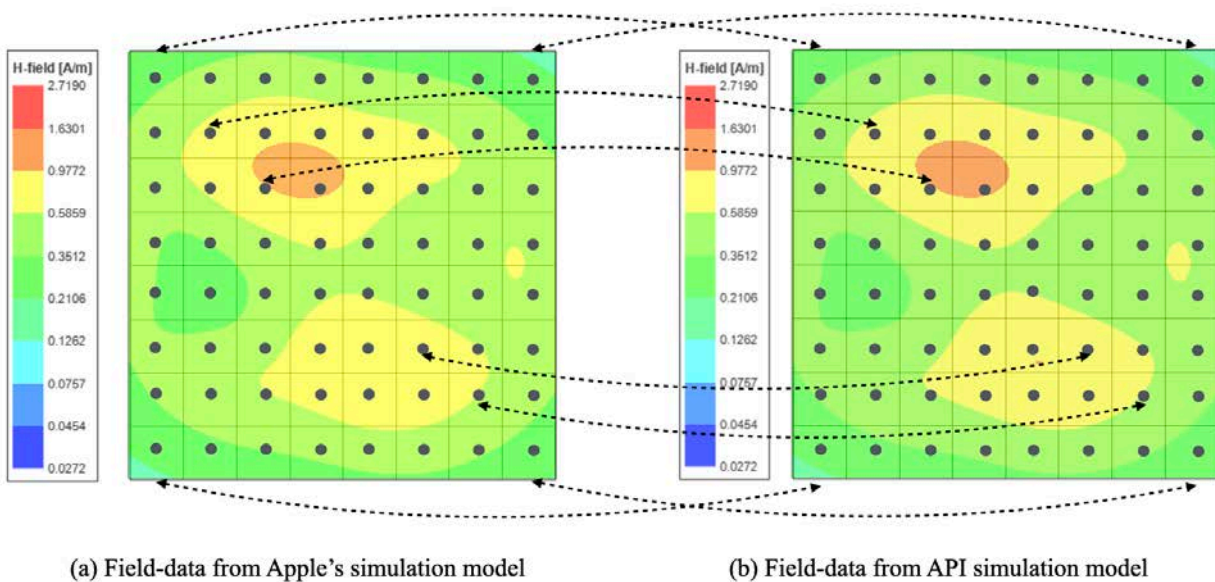


Figure 11: Sample Field Plots to Show the Field Data Comparison Between Two Plots

An additional report with detailed analysis on validation of Watch Charger simulation model will be included in the vendor's SAR compliance report. In the validation report, both E and H fields are compared using the procedure described above for both the maximum and minimum coupling cases.

The verified simulation model is then used for SAR calculations with a phantom added in contact with the EUT along with third party housing and other relevant geometries.

5.2 SAR Simulations

API interface accepts only 3D CAD geometry as input. Users do not have access to modify the WPT module parameters such Tx Coil and Rx Coil parameters, spacing etc...Vendors can only add external CAD housing geometries. The working of API interface is shown in Fig. 12.

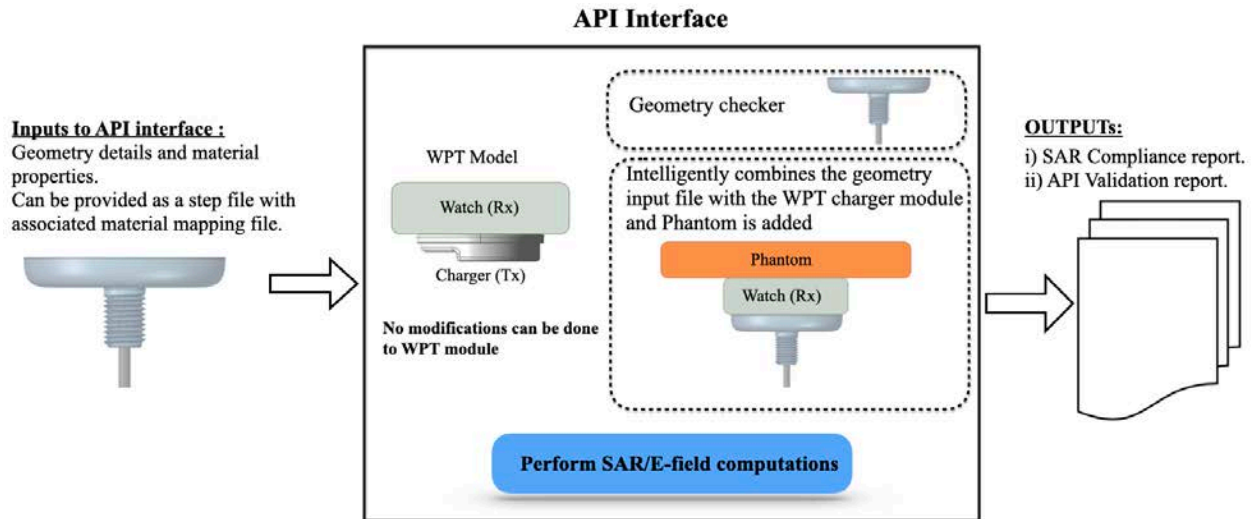


Figure 12: Example to Demonstrate the Working of API Interface

Inputs to API interface: Third party vendors can add custom housing and other relevant CAD geometries to represent the device accurately to perform the computational SAR assessment studies. A 3D CAD geometry file and a material mapping file can be provided as input to the API interface. SAR Compliance Report to be submitted by the vendor will include all the details about the geometry and the material properties of the CAD housing used for SAR simulations. Detailed list of inputs that will be provided by the Vendor to the API interface is listed in the below Table 8.

Table 8. List of inputs to API interface

Item	Description
1	Model No. of EUT
2	EUT's FCC ID
3	Vendor Company Details: Name, Location
4	Date of Simulation: Date when simulation request is submitted to API interface
5	EUT Description
6	External CAD Housing details: 3D CAD geometry file (such as STEP file) which includes custom form factor housing, dielectrics, and any additional cable routing with their associated material properties

Geometry Checker: The purpose of this step is to make sure that only valid geometry is provided as input to the API. Geometry checker verifies the following criteria:

- i. Only solid objects are present.

- ii. No geometry intersections with the charger module.
- iii. Valid material properties are assigned to the objects.

If any of the conditions are not met, a detailed feedback is provided to the user.

After the geometry check stage is passed, a Phantom with the correct material properties and size is added to simulate all the exposure test cases listed below.

5.3 SAR Compliance Results:

Two exposure cases i) Max Coupling and ii) Max offset, cases are selected for SAR investigation. Considering that the phantom can be in contact with the watch or charger, there is a total of four scenarios.

Exposure Case 000 (a): Nominal configuration with perfect alignment and phantom placed above the receiving unit.

Exposure Case 000(b): Nominal configuration with perfect alignment and phantom placed below the transmitting unit.

All simulations are performed at 0 mm spacing between EUT and phantom in all scenarios mimicking on-body use case, therefore the worst case is being considered. By using the worst-case orientation for simulation (on-body) all other SAR scenarios will have less SAR values (Head, extremities, and desktop) .

5.3.1 Additional Exposure Cases:

Two unrealistic cases where the charger is in direct contact with the phantom are investigated. Worth mentioning that these cases do not happen in real-life applications.

Unrealistic (Theoretical) Exposure Case 1(a): Unrealistic worst-case configuration with receiving unit absent and phantom placed above the transmitting unit.

Unrealistic (Theoretical) Exposure Case 1(b): Unrealistic worst-case configuration with receiving unit absent and phantom placed below the transmitting unit.

For all the exposure cases, dielectric properties (conductivity and permittivity) used for the phantoms are fixed as (permittivity: 5016, conductivity: 0.5).

The coil properties are also fixed, transmitting coil with 11 turns and measures 7.5 uH nominally in free air. The receiver coil consists of 13 turns and measures 9.06 uH nominally in free air.

Both coils are wound spirally.

The following outputs are calculated and reported in the Table:

- a. Peak spatial 1-g average SAR in tissue.
- b. Peak RMS spatial electric field in tissue.

SAR simulation results for all the above scenarios will be included in the SAR Compliance Simulation Report to be submitted by the third-party vendor. Sample SAR simulation report is included in the appendix for reference.

6 Summary

Based upon the above description, the simulation model is shown to be a proven framework for third-party vendors to assess SAR compliance.

7 Annex A: Specific Information for SAR Computational Modelling

1) Computation Resources

The models were simulated on a 96 core CPU server with an available RAM of 4 Terabytes. Each model variation took around 12 hours to complete. Based on the simulation profile, the minimum resources needed to finish these simulations will be approximately 8 core CPU with 512 GB of RAM. Using the minimum requirements simulation will likely take more time than 12 hours.

2) Computational parameters

The table below show the most important parameters used in the SAR calculations. Some of these parameters have been varied and the uncertainty variations are reported in section 4.

Table 9. List of Computational Parameters

Parameter	Value
Smallest FEM Mesh size	Edge = 0.000689 mm
	Volume = 1.429e-13 mm ³
Domain Size	2572 mm by 3700 mm by 2951 mm
Tissue-EUT separation	0 mm
Tissue ϵ_r	5016
Tissue Sigma	0.5
EUT to ABC Distance	1260 mm
Max Delta Energy Convergence Criterion	0.1

In H-field and SAR simulations we are using current sources to excite the coils. Therefore, the convergence metric in HFSS is defined based on Maximum Delta Energy. Ansys HFSS help document states that “the Delta Energy is the difference in the relative energy error from one adaptive solution to the next. It is a measure of the stability of the computed field values from pass to pass.” We set the Max Delta Energy Convergence Criterion to 0.1 and based on our knowledge and experience this number would usually provide a good balance between the speed

and accuracy. Worth mentioning that we also force a minimum number of passes condition for the convergence (e.g., 5). This means that the solver stops the adaptive meshing process only if both of these two criteria are satisfied. Therefore, the final converged solution may have a Maximum Delta Energy well below the set value of 0.1.

3) Tx and Rx coil parameters

Both Coils were driven using lumped ports. Each coil had two lumped ports assigned at each end. The current driving the coils were assigned differentially between the two ports per use case. Below is a table describing some parameters for TX and RX coils.

Table 10. Tx and Rx Coil Parameters

	RX Coil	TX Coil
Winding Type	Spiral, 2 Layers, Stranded Wire	Spiral, 1 Layer, Stranded Wire
Turns	6	9
Inner Radius	8.36 mm	7.5 mm
Outer Radius	9.45 mm	10.2 mm
Cross section	Circular	Circular
Wire radius	0.13 mm	0.1 mm

4) Phantom model implementation and validations

Eli phantom was chosen to represent Body case. The size of the phantom is shown below:

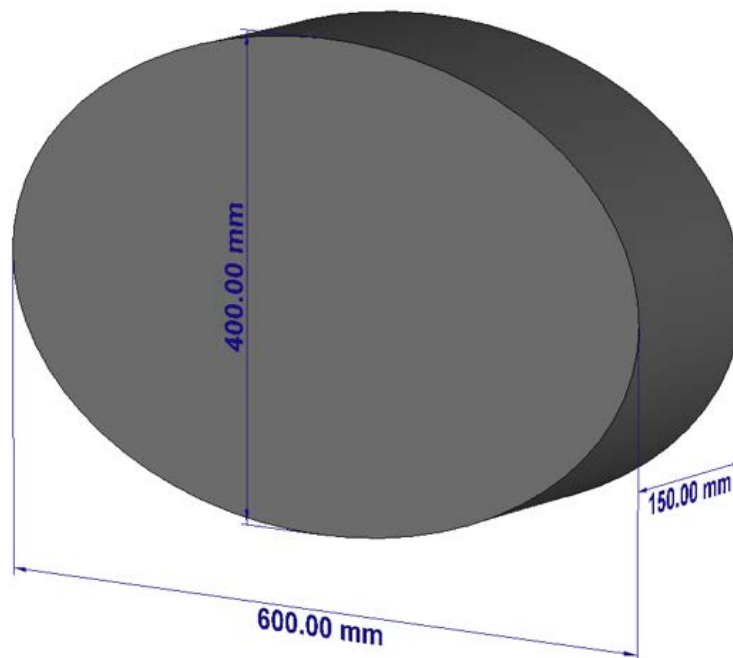


Figure 13: Phantom Dimensions

The material properties used in the phantom is disused in section 5. HFSS mesh adaption was used to make sure the SAR value converges.

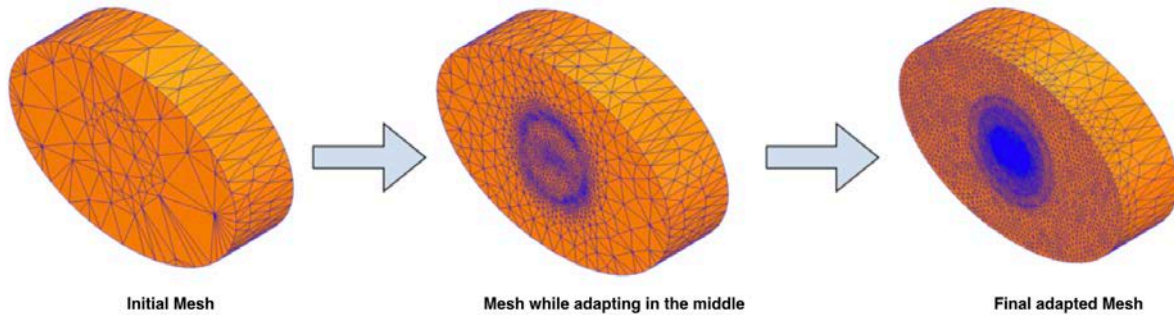


Figure 14: Adaptive Meshing in HFSS

5) Transmitter model implementation and validation

As described in the main section, H-field measurements were used to validate the transmitter model. The same transmitter model was shared with third-party vendors for SAR assessments. Below is the simulations vs. measurements comparison.

Simulated Vs Measured H-field Comparison

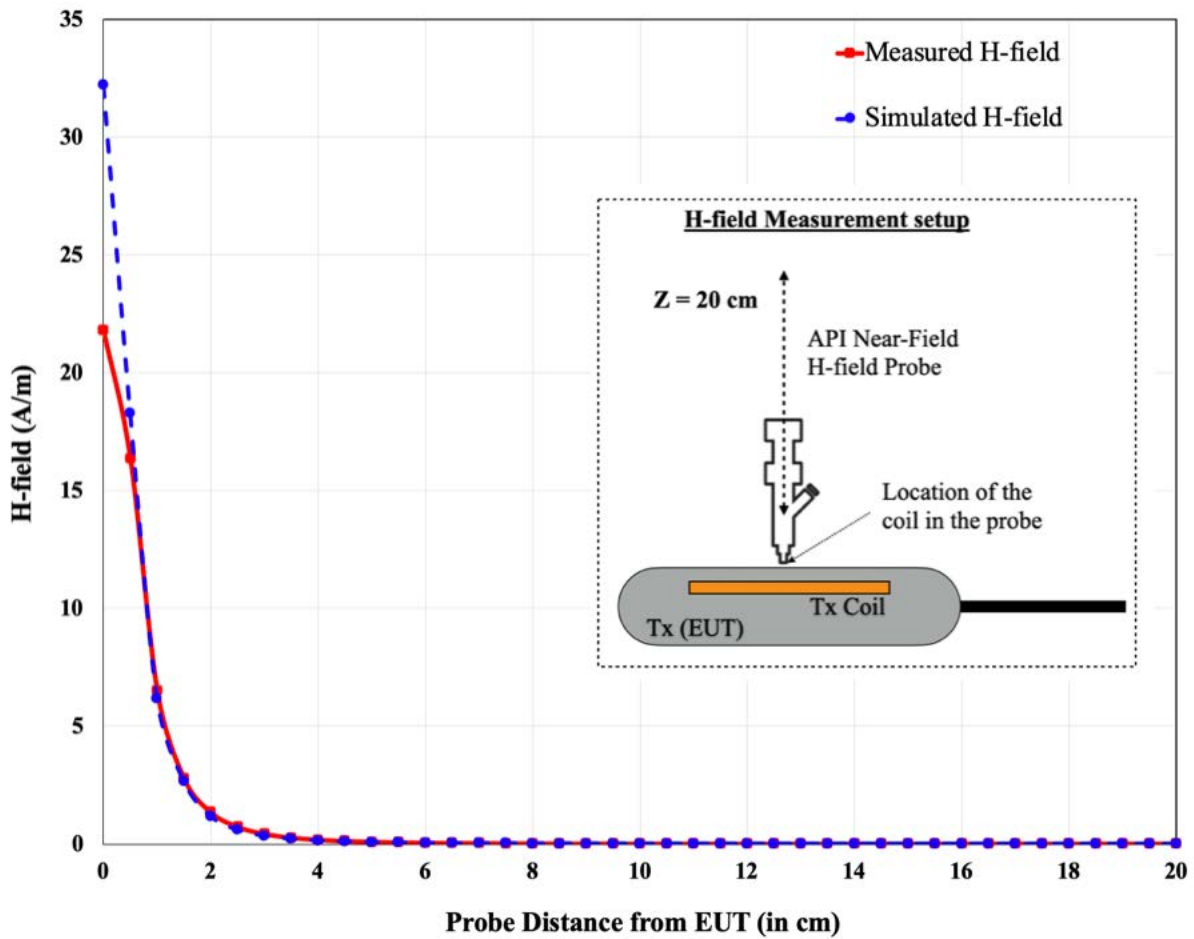


Figure 15: Simulated Vs Measured Correlation of Transmitter model

6) Steady state termination procedure

S-parameter convergence is used to determine the stability of the model. By default, HFSS uses 0.02 of convergence criteria. Convergence was changed to 0.002 to make sure the problem converged well. On top of convergence criteria, the surface of the phantom facing the EUT was seeded for more dense mesh as shown below.

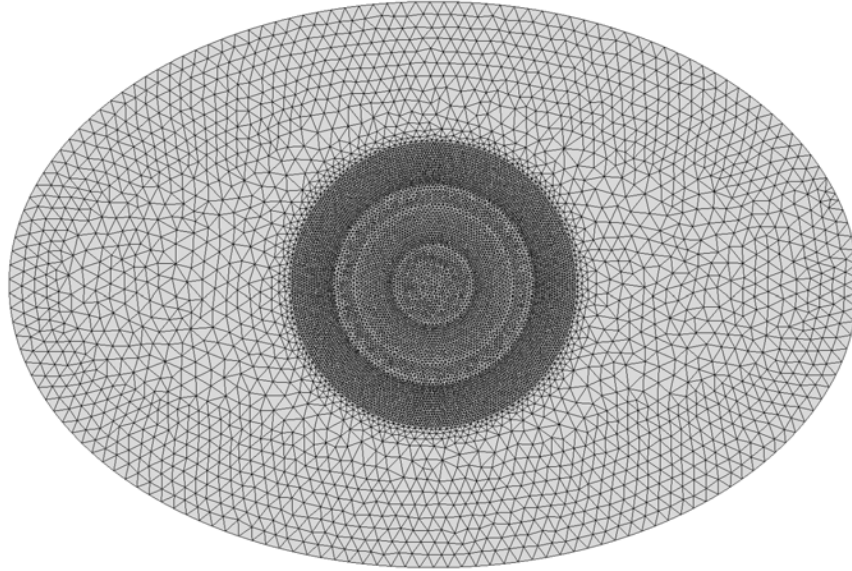


Figure 16: Mesh Seeding on Phantom

Combining those two methods, we believe the model is converging well to capture the steady-state values of SAR.

7) Computational peak SAR from peak components & One-gram averaged SAR procedure

The calculation method for SAR follows IEEE P1528.4. Once the solver calculated the S-Parameter results, different coils can be driven and the result from the S-Parameter calculation is automatically scaled to the driving current of the coils. This result combination provides the correctly scaled power loss density in the phantom. The SAR calculation computes the local SAR first using electric field and conducting current:

$$SAR = \vec{E} \bullet \vec{J}_{conj} / (2\rho)$$

Afterwards the local SAR is averaged over a specific mass, usually 1 g or 10 g. As described in [IEEE P1528.4] the mass averaging is done by mapping the results to a structured hexahedral grid and afterwards the averaging scheme for FDTD per [IEEE P1528.4] is applied. The SAR calculation on the hexahedral grid is compliant with IEC 62704-1.

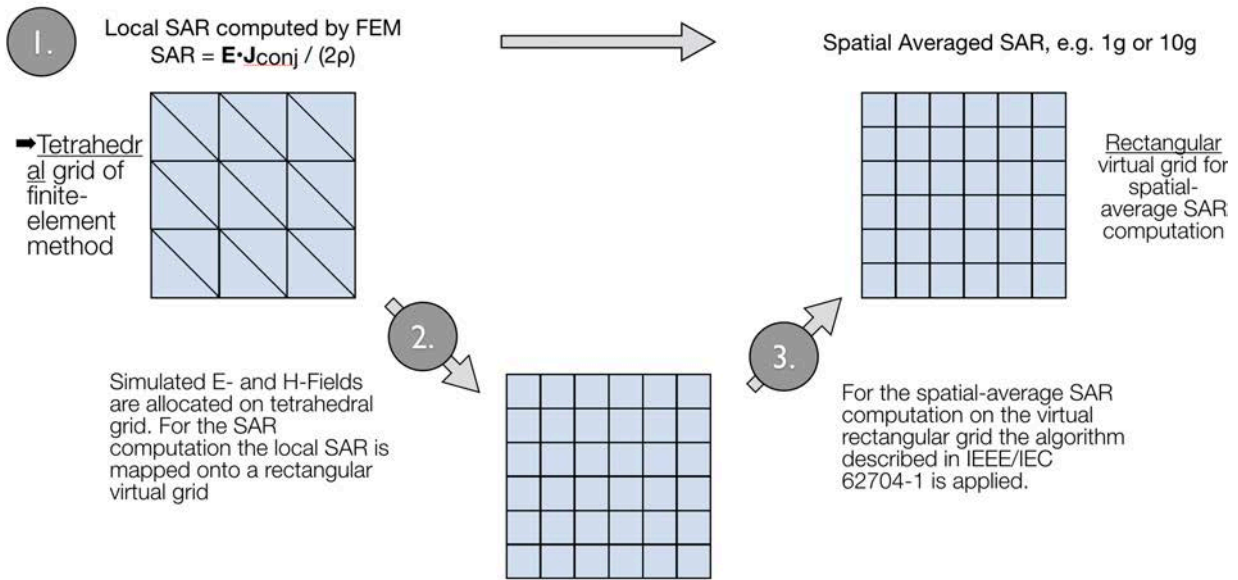


Figure 17: IEEE P1528.4 for SAR Computation

8 Annex B: Algorithm Validation and Benchmarks

This section is divided into two parts. The code performance validation provides methods to determine that the finite-element algorithm in HFSS has been implemented correctly and works accurately within the constraints due to the finite numerical accuracy. It further determines the quality of absorbing boundary conditions and certain parts of the post processing algorithms that are part of HFSS. The second part has few canonical benchmarks. All benchmarks can be compared to analytical solutions of the physical problem or its numerical representation. The methods characterize the implementation of the finite-element algorithm used by HFSS in a very general way. They are defined such that it is not possible to tune the implementation for a particular benchmark or application without improving the overall quality of the code.

2.1) Code Performance Validation

2.1.1) Propagation Homogeneous Medium

A straight rectangular waveguide with ports on both ends is well suited as a first test of an implementation of the Finite-Element Method used by HFSS. The waveguide has a width of 20 mm, a height of 10 mm and a length of 300 mm. The waveguide is filled homogeneously with a material which, in three separate simulations, shall assume the following properties:

- $\epsilon_r = 1, \sigma = 0 \text{ S/m};$
- $\epsilon_r = 2, \sigma = 0 \text{ S/m};$
- $\text{Re}(\epsilon_r) = 2, \sigma = 0.2 \text{ S/m}.$

To verify that the mesh used by HFSS is independent of orientation, the waveguide has been rotated so that it is not parallel with any principal coordinate plane (XY, XZ, YZ). The waveguide is driven in the TE₁₀ mode at 10 GHz. Reported are the magnitudes of S₂₁ and S₁₁, as well as the values of the real and imaginary parts of the propagation constant γ . The table below provides the reference values [B1], acceptable result criteria, as well as the simulated results.

Criteria for the Waveguide Evaluation

Re(ϵ_r)	1	2	2
σ	0	0	0.2
S ₂₁ reference value	1	1	8.7×10^{-5}
Criterion for S ₂₁	≥ 0.9999	≥ 0.9999	$\pm 5 \times 10^{-6}$
S ₂₁ simulated results	1	1	8.7×10^{-5}
S ₁₁ reference value	0	0	0
Criterion for S ₁₁	≤ 0.003	≤ 0.003	≤ 0.003
S ₁₁ simulated results	0	0	0
Re(γ) reference value	0	0	31.17 m^{-1}
Criterion for Re(γ)	$\pm 0.1 \text{ m}^{-1}$	$\pm 0.1 \text{ m}^{-1}$	$\pm 2\%$
Re(γ) simulated results	0	0	31.17
Im(γ) reference value	138.75 m^{-1}	251.35 m^{-1}	253.28 m^{-1}
Criterion for Im(γ)	$\pm 2\%$	$\pm 2\%$	$\pm 2\%$
Im(γ) simulated results	138.75	251.35	253.28

As is seen in the above table, HFSS easily meets the criteria for properly and accurately calculating the waveguide problem.

2.1.2 Planar Dielectric Boundary

In order to test the reflection of a plane wave by a dielectric boundary, a rectangular waveguide can again be used. It is well known that the TE₁₀ mode can be thought of as a superposition of two plane waves [B1]. Each wave's direction of propagation makes an angle θ with the axis of the wave guide, given by

$$\cos^2\theta = 1 - (c/2af)^2 \quad (1)$$

where c is the speed of light, a is the width of the wave guide and f is the frequency. Assuming the axis of the waveguide is the Z axis and assuming the waveguide is filled with vacuum for $Z > 0$ and filled with dielectric 1 with complex relative permittivity ϵ_r for $Z < 0$, Fresnel reflection coefficients for the TE and the TM cases, defined as ratios of electric field strengths, are given by [B2]

$$R^{\text{TE}} = (k_{0,z} - k_{1,z}) / (k_{0,z} + k_{1,z}) \quad (2)$$

$$R^{\text{TM}} = (\epsilon_r k_{0,z} - k_{1,z}) / (\epsilon_r k_{0,z} + k_{1,z}) \quad (3)$$

where $k_{0,z}$ and $k_{1,z}$ denote the z component of the propagation vector of the plane wave in vacuum and in the dielectric, respectively. They can be evaluated through

$$k_{0,z} = k_0 \cos\theta \quad (4)$$

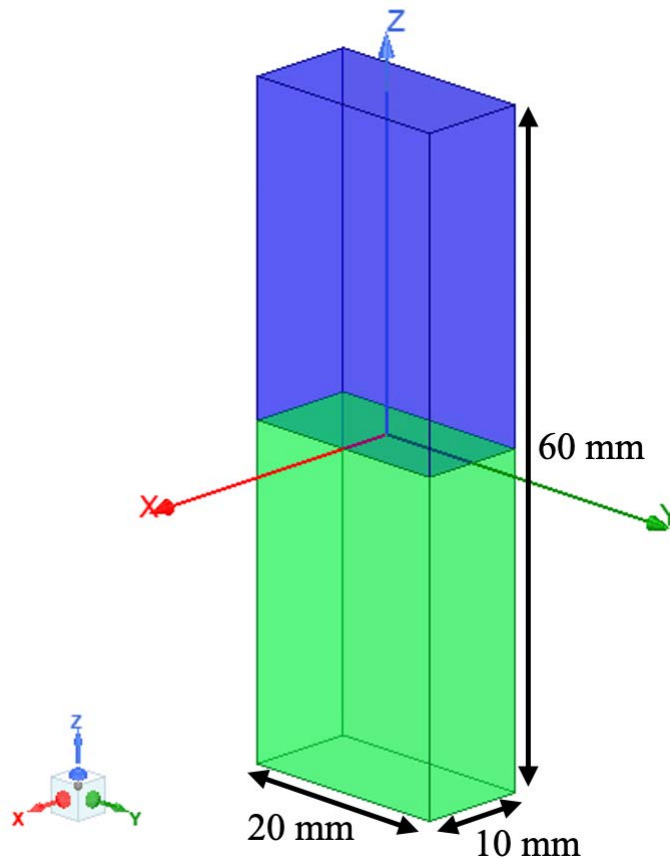
$$k_{1,z} = k_0 \sqrt{\epsilon_r - \sin^2\theta} \quad (5)$$

Finally, ϵ_r is complex and is given by

$$\epsilon_r = \text{Re}(\epsilon_r) - j\sigma/(2\pi f\epsilon_0) \quad (6)$$

where $\text{Re}(\epsilon_r)$ denotes the real part of the relative permittivity, σ is the conductivity of the medium, and ϵ_0 is free space permittivity 8.85×10^{-12} F/m.

For this test, a $20 \text{ mm} \times 10 \text{ mm}$ waveguide with a length of 60 mm , as shown below, was created. The top half was filled with vacuum and the bottom half with dielectric.



Waveguide Filled Half with Vacuum and Half with Dielectric

In one copy of the model, all side walls were lossless metal, such that the dominant mode is the TE₁₀ mode with propagation constant 138.75 m⁻¹ at 10 GHz and represents the TE case in the reflection analysis. In the other copy of the model, the side walls that are parallel to the YZ plane were perfect magnetic conductors while the other walls were perfect electric conductors, such that the second mode (after a TEM mode which won't be used in this test) has propagation constant 138.75 m⁻¹ at 10 GHz and represents the TM case in the reflection analysis.

Before simulation, the waveguides were rotated over an arbitrary angle such that no face is parallel with any coordinate plane. The waveguides were driven at 10 GHz in the proper mode. In doing so, it is good practice to calculate all propagating modes, but the coupling between modes is expected to be negligible. Simulations were run for the cases of lossless and lossy dielectric as shown in the next table. For the HFSS to pass the test, according to IEC 62704-1, the results need to be within 2% of the analytical values.

Reflection at a Dielectric Interface

Re(ϵ_r)	σ (S/m)	RTE	RTE- Simulated	RTM	RTM - Simulated
4	0	0.4739	0.4739	0.1763	0.1763
4	0.2	0.4755	0.4755	0.1779	0.1779
4	1	0.5105	0.5105	0.2121	0.2121

As can be seen from the data, HFSS produces results identical to the analytical values.

2.2) Canonical Benchmarks

The results for few low frequency benchmarks are summarized below. These benchmarks were used to validate the accuracy of the tool at low frequencies:

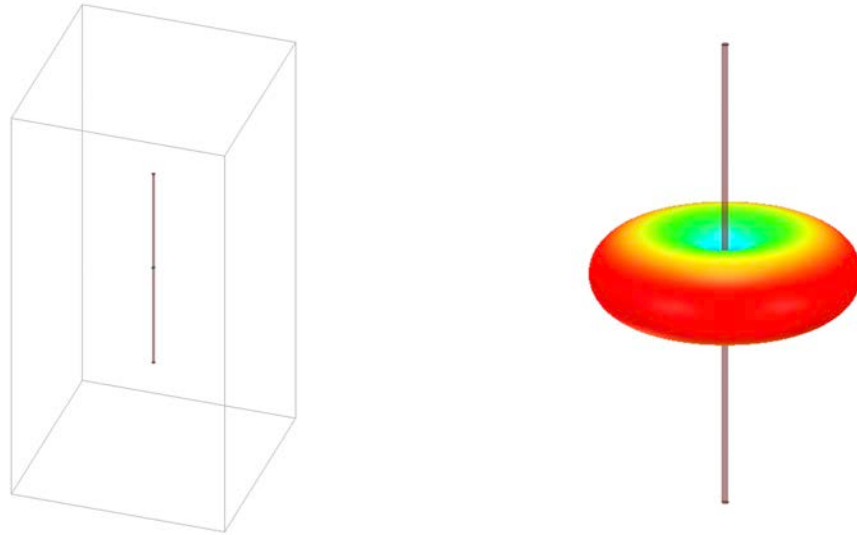
2.2.1) Dipole Antenna:

The following parameter were used to design a dipole antenna to resonate at 400 kHz.

Dipole length: 375 meters

Feed gap: 2.5 meters

Dipole diameter: 5 meters



Dipole Antenna Model

IEC 62704-4 ED1 was referenced to compare the tables. Two computation methods were demonstrated as shown below to show the validity of the model.

Simulated Dipole Parameters

FEM Solver

Quantity	Simulation results	Tolerance	Satisfied?
Re (Z) at 400 kHz	94.26		
Im (Z) at 400 kHz	57.45		
Re (Z) at 320 kHz	39.4	$25\Omega < Re(Z) < 50\Omega$	Yes
Im (Z) at 320 kHz	-91.75	$-50\Omega < Im(Z) < -100\Omega$	Yes
Re (Z) at 360 kHz	59.81	$50\Omega < Re(Z) < 75\Omega$	Yes
Im (Z) at 360 kHz	-18	$-25\Omega < Im(Z) < 0\Omega$	Yes
Frequency for Im (Z) = 0	369.6	$360\text{ kHz} < f < 380\text{ kHz}$	Yes
Maximum power budget error	0.3	$< 5\%$	Yes

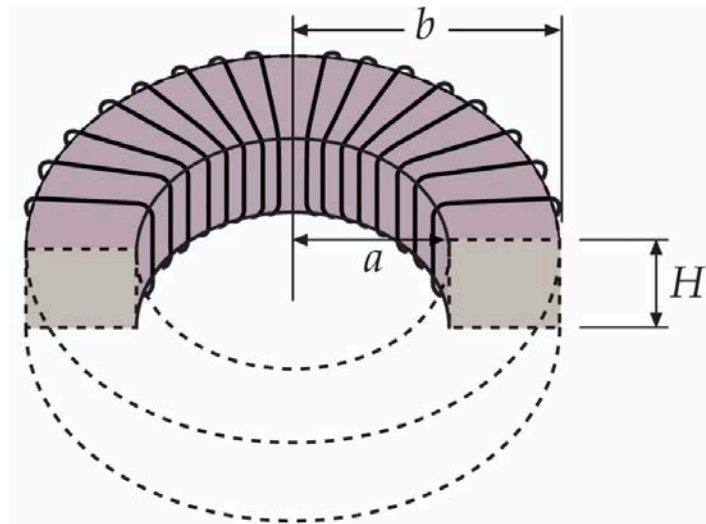
MoM Solver

Quantity	Simulation results	Tolerance	Satisfied?
Re (Z) at 400 kHz	93.9		
Im (Z) at 400 kHz	56.5		
Re (Z) at 320 kHz	40.95	$25\Omega < Re(Z) < 50\Omega$	Yes
Im (Z) at 320 kHz	-89.6	$-50\Omega < Im(Z) < -100\Omega$	Yes
Re (Z) at 360 kHz	61.25	$50\Omega < Re(Z) < 75\Omega$	Yes
Im (Z) at 360 kHz	-17.6	$-25\Omega < Im(Z) < 0\Omega$	Yes
Frequency for Im (Z) = 0	369.6	$360\text{ kHz} < f < 380\text{ kHz}$	Yes
Maximum power budget error	0.4	$< 5\%$	Yes

2.2.2) Toroid Inductor:

A toroid was simulated using the below dimensions and the cross-section of the toroid is shown in the below figure.

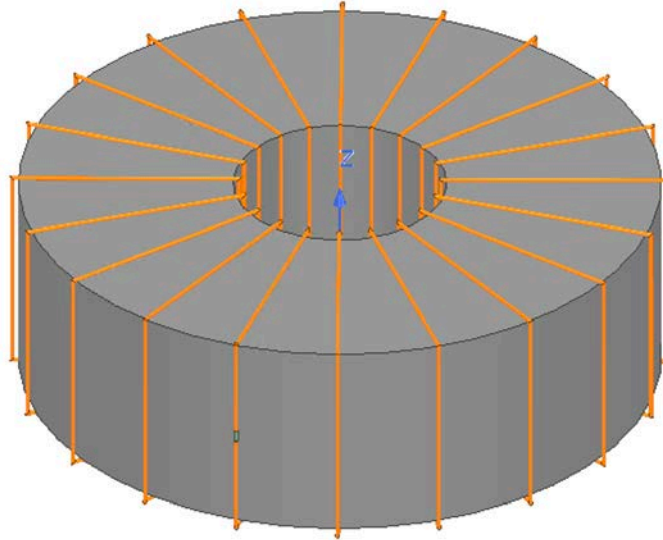
- Total number of turns (N) = 20
- Inner radius (a) = 13 mm
- Outer radius (b) = 39 mm
- Height (H) = 25 mm
- Magnetic permeability (μ_r) = 64



Expression used to compute Inductance is given below [6,7].

$$L = \frac{\mu N^2 H}{2\pi} \ln\left(\frac{b}{a}\right)$$

The formula gave an inductance of 140.6 uH. The model created in HFSS gave an inductance of 141.6 uH. The difference is less than 0.7%.



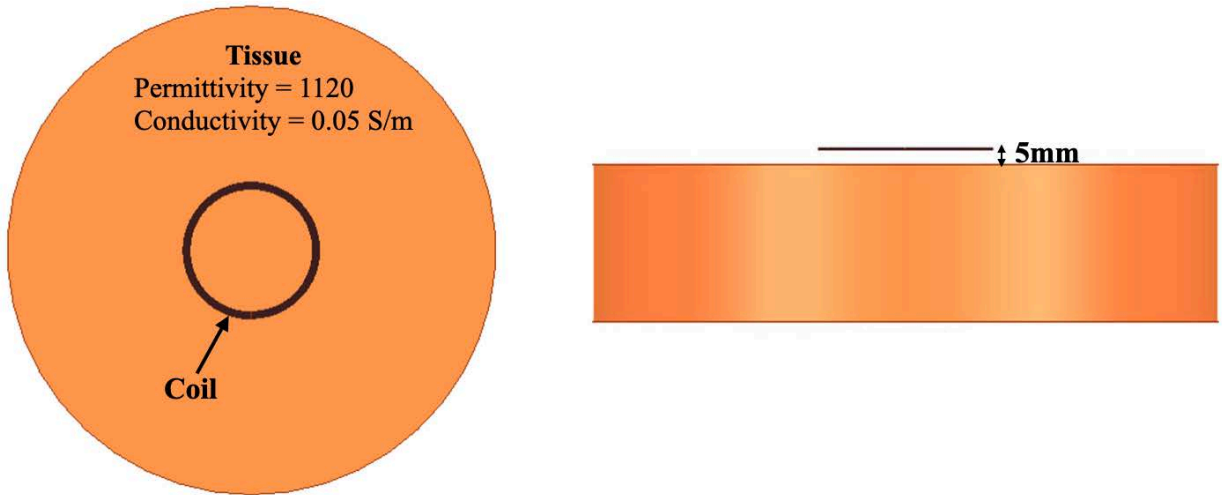
Toroid Model in HFSS

2.2.3) Circular Coil Parallel to a Flat, Homogeneous Phantom.:

The following benchmark is implemented using Equations 1-4 from Chen et al [8].

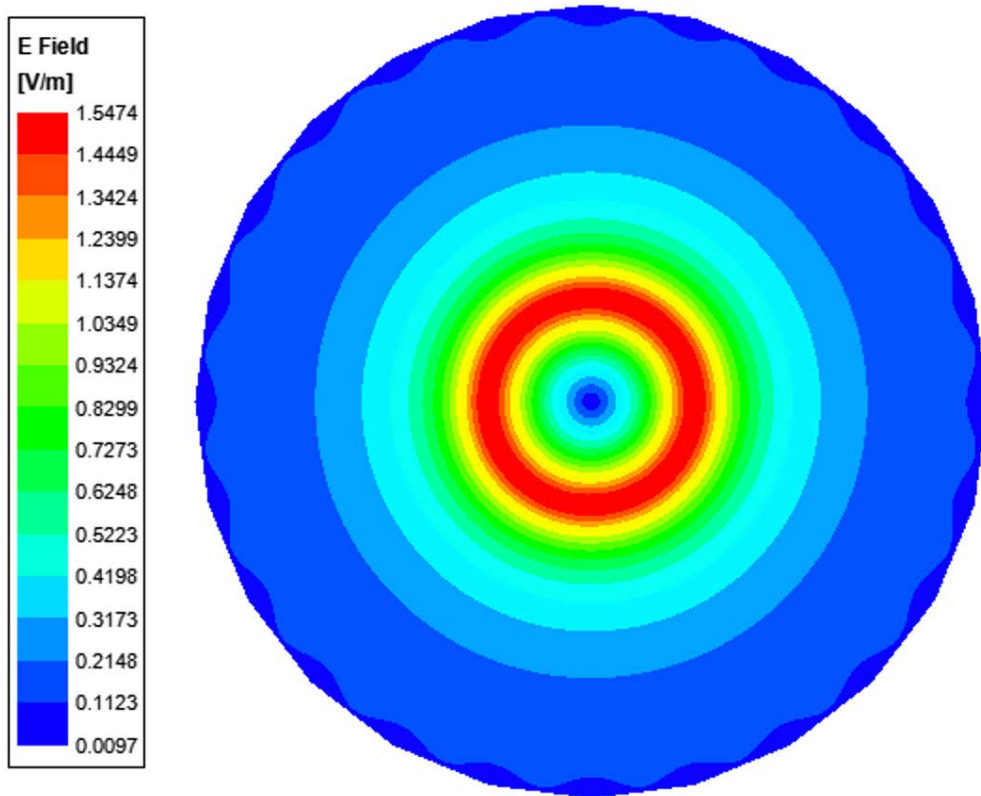
Below is the coil and phantom parameters:

- Coil Inner radius: 25 mm
- Coil Outer radius: 28 mm
- Number of Turns: 10
- RMS Current: 0.707 A (peak current = 1 A)
- Frequency: 100 kHz
- Coil-to-Body Distance: 5 mm
- Tissue Conductivity: 0.05 S/m
- Tissue Permittivity: 1120



Circular Coil in front of Tissue

The simulated spatial peak RMS electric field in tissue is 1.54 V/m compared to the analytical value of 1.52 V/m.



Electric field Plot

9 Annex C: Human Tissue Modeling

Human Tissue Material Properties at 326 kHz and 1.778 MHz:

The worst-case scenario has been identified to be when a user is holding the device in hand and taking a call or holding the watch on their body while charging. The electrical properties for body and hand layers are shown below. Since the SAR phantom is homogenous, using the layers' properties, the worst-case scenario is selected and applied for the phantom properties. Therefore, for the SAR simulations, the phantom that has conductivity of 0.5 and permittivity of 5016 at the 326 kHz and 1.778 MHz operating frequency is used. In addition, mass density of 1000 Kg/m³ was used.

Electrical Properties:

Based on our research this is what we recommend for ϵ_r and sigma values for body layers

Table 11. Electrical Properties for Body Layers

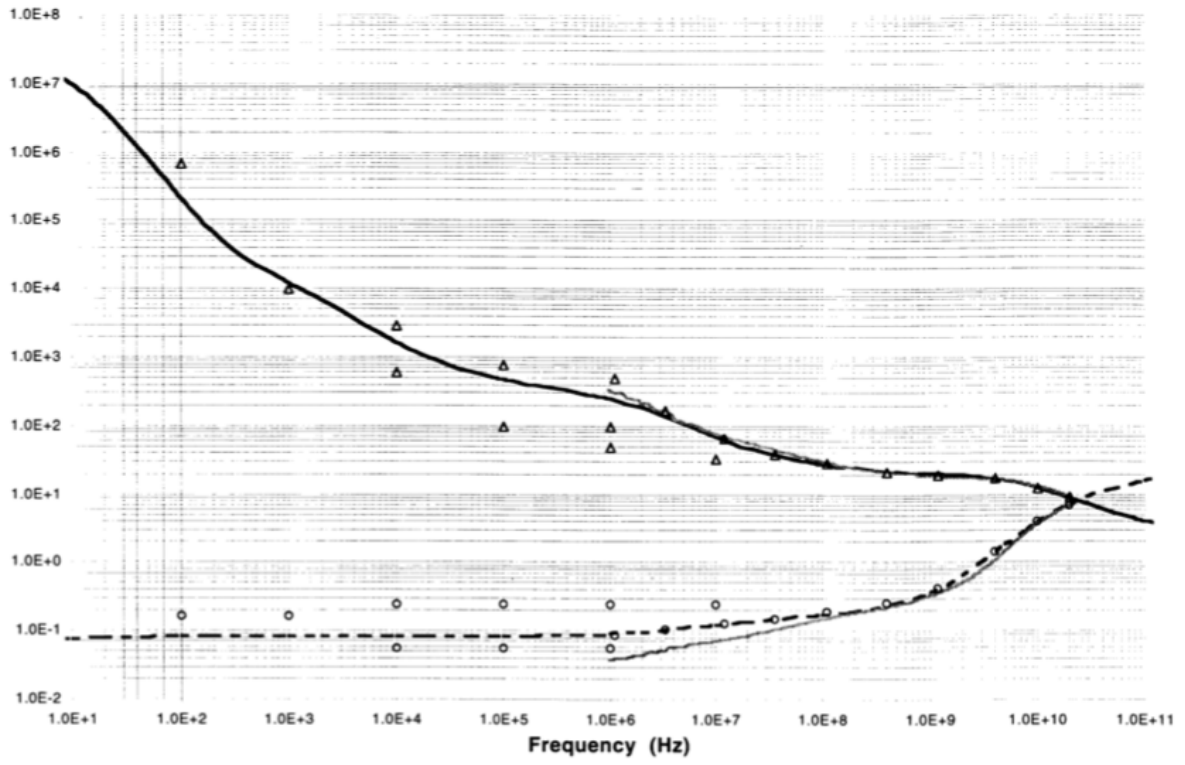
Tissue	Thickness (mm)	Permittivity	Conductivity (S/m)
Skin	3	5016	0.16
Muscle	9	4666	0.5
Bone	20	1414	0.165
Worst case	100	5016	0.5

Based on our research, this is what we recommend for ϵ_r and σ values for hand layers.

Table 12. Electrical Properties of Human Hand Layers

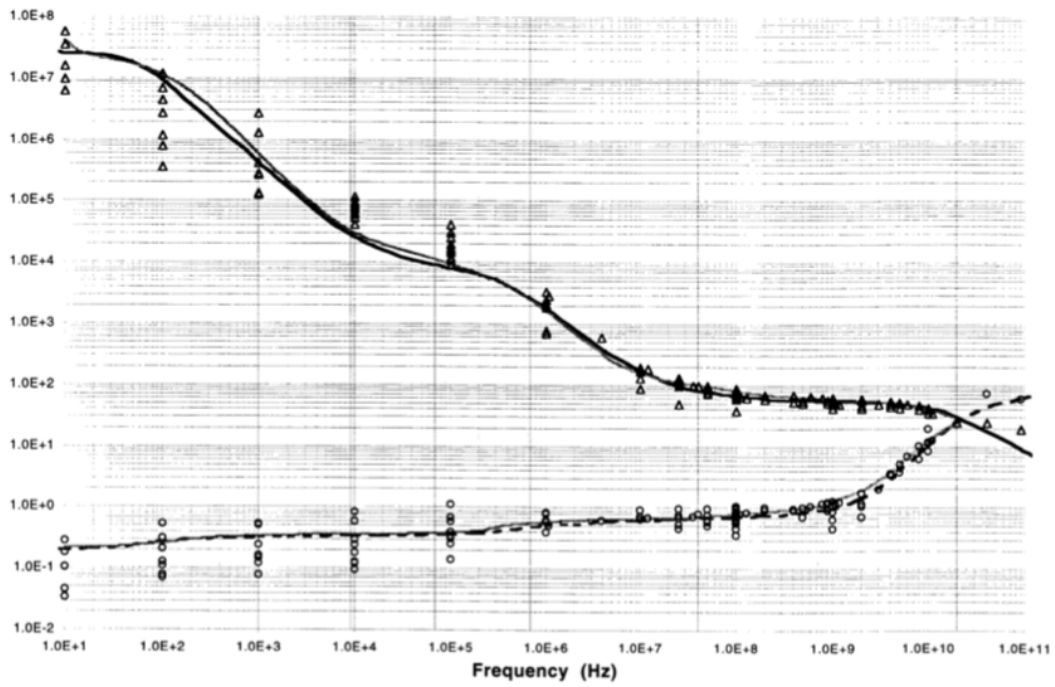
Tissue	Thickness (mm)	Permittivity	Conductivity (S/m)
Skin	2	5016	0.16
Muscle	2	4666	0.5
Bone	15	1414	0.165
Worst case	100	5016	0.5

Bone (Cancellous)

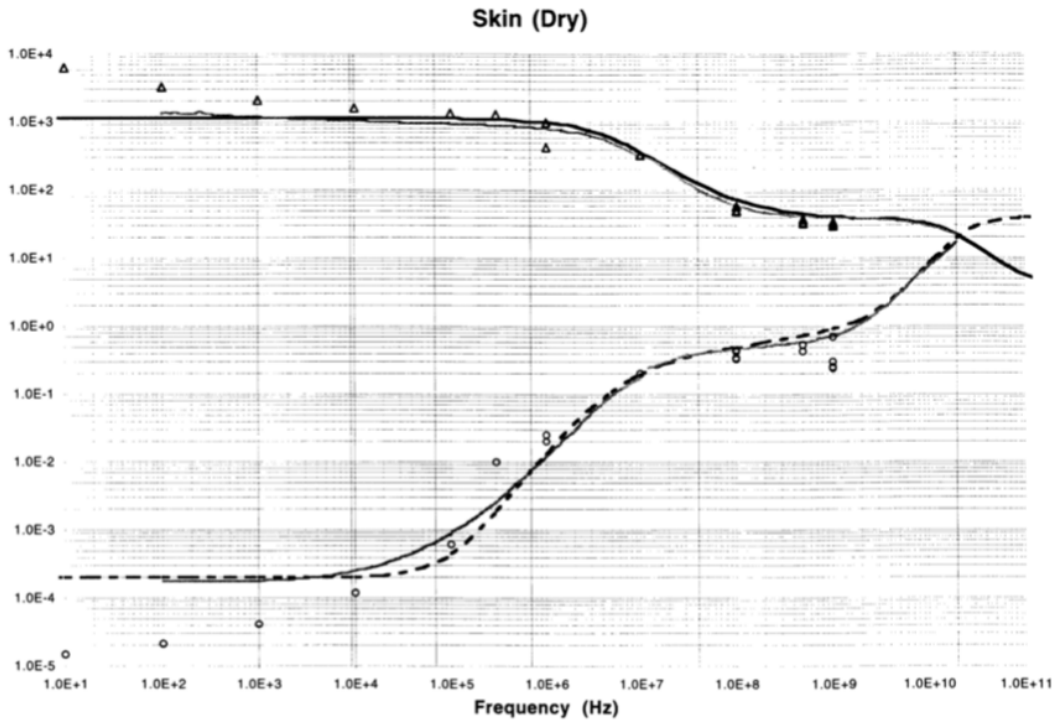


(a)

Muscle



(b)



(c)
 Figure 18: Electrical Properties of (a) Bone, (b) Muscle, and (c) Dry Skin

References:

- 1) http://amberpi.com/products_EMI_probes.php
- 2) The electrical conductivity of human cerebrospinal fluid at body temperature, S.B. Baumann ; D.R. Wozny ; S.K. Kelly ; F.M. Meno, IEEE Transactions on Biomedical Engineering (Volume: 44 , Issue: 3 , March 1997)
- 3) C.Gabriel, S.Gabriel and E.Corthout: The dielectric properties of biological tissues: I. Literature survey, Phys. Med. Biol. 41 (1996), 2231-2249.
- 4) S.Gabriel, R.W.Lau and C.Gabriel: The dielectric properties of biological tissues: II. Measurements in the frequency range 10 Hz to 20 GHz, Phys. Med. Biol. 41 (1996), 2251-2269.
- 5) S.Gabriel, R.W.Lau and C.Gabriel: The dielectric properties of biological tissues: III. Parametric models for the dielectric spectrum of tissues, Phys. Med. Biol. 41 (1996), 2271-2293.
- 6) <https://itis.swiss/virtual-population/tissue-properties/database/thermal-conductivity/>
- 7) <http://www.phys.uri.edu/gerhard/PHY204/tsl267.pdf>
- 8) <http://web.mit.edu/viz/EM/visualizations/notes/modules/guide11.pdf>
- 9) X. L. Chen et al., "Human Exposure to Close-Range Resonant Wireless Power Transfer Systems as a Function of Design Parameters," in IEEE Transactions on Electromagnetic Compatibility, vol. 56, no. 5, pp. 1027-1034, Oct. 2014.